TITANIUM-IN-QUARTZ GEOTHERMOMETRY OF IMPACTITES AND PEAK-RING LITHOLOGIES FROM THE CHICXULUB IMPACT CRATER. Martin Schmieder[1,2], D. Kent Ross[3], Katharine L. Robinson[1,2] and David A. Kring[1,2], [1]Lunar and Planetary Institute – USRA, Houston, TX 77058 USA (schmieder@lpi.usra.edu), [2]NASA–Solar System Exploration Research Virtual Institute (SSERVI), [3]University of Texas El Paso/Jacobs Technology/NASA–JSC–ARES, Houston, TX 77058 USA.

Introduction: Since its development by Wark and Watson (2006) [1], the Ti-in-quartz geothermometer (TitaniQ) has been continuously refined and applied to a variety of lithologies from different crustal settings. Assuming quartz crystallized and incorporated Ti under equilibrium conditions and providing TiO_2 activity (a_{TiO_2}) is reasonably constrained, crystallization temperatures at typical crustal pressures can be calculated. In turn, when crystallization temperatures are independently constrained, Ti-in-quartz can be used as a geobarometer [2-10].

Here we explore the application of this technique to impact lithologies. Quartz is ubiquitous in terrestrial impact structures in upper crustal settings and can also form as a post-impact hydrothermal mineral [11]. Together with other geothermometers, such as Ti-in-zircon [12,13], Ti-in-quartz can potentially help constrain the temperature–pressure conditions during the formation of the pre-impact target rock at terrestrial impact structures, as well as impact-produced and hydrothermally-altered lithologies. This work presents the first systematic Ti-in-quartz study of impactites and granitoid target rocks from the ~180 km-diameter, end-Cretaceous Chicxulub crater on the Yucatán Peninsula, Mexico, thereby placing new constraints on the emplacement of felsic plutons within the Maya Block [14] in the Paleozoic, impact melt crystallization [15-17] at ~66 Ma, and post-impact hydrothermal overprint [18-21] inside the Chicxulub crater.

Samples and Analytical Techniques: One polished thin-section from the PEMEX Yucatán-6 (Y-6) borehole inside the annular crater moat surrounding Chicxulub's peak ring [16,17] and five polished thin-sections of rock samples from the IODP–ICDP Expedition 364 borehole into the peak ring and overlying lithologies (drill core M0077A) [22,23] were analyzed for trace amounts of Ti and Al. The Y-6 sample (Y6-N19-11b) is a clast-rich impact melt rock cross-cut by a ≤5 mm-wide secondary vein and pockets of spherulitic silica intergrown with euhedral anhydrite (Fig. 1), from a depth of 1377–1379.5 m below sea level [14-17]. Samples from the Expedition 364 core include reworked and hydrothermally-altered, melt-bearing breccia (henceforth referred to as suevite) that is cemented by a carbonate–quartz–zeolite groundmass (sample 47-1-48-60, core depth 638 m below sea floor [mbsf]), and a selection of shocked and uplifted granitoid rocks from the peak ring (samples 150-3-25.5-27 from 887 mbsf; 174-2-19-20 from 949 mbsf; 237-2-60-61.5 from 1133 mbsf; and 276-1-85-87 from 1250 mbsf) [22,23]. Silica in the Y-6 melt rock and the Expedition 364 suevite contains Ti-magnetite, whereas the granitoid target rocks from the peak ring contain magmatic titanite. None of the samples analyzed have rutile as the primary Ti-carrier phase.

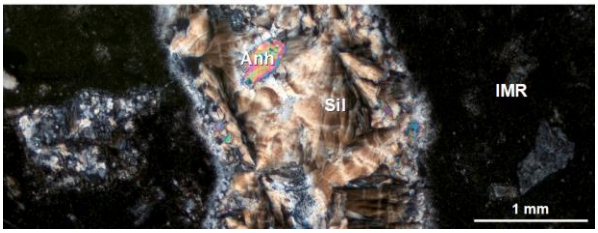

Fig. 1: Secondary vein of silica (Sil) and anhydrite (Anh) cross-cutting impact melt rock (IMR) (sample Y6-N19-11b) from the Yucatán-6 borehole. Cross-polarized light.

Electron microprobe analysis (EMPA) was carried out using a JEOL JXA-8530F field emission electron microprobe at the NASA Johnson Space Center (15 kV accelerating voltage; beam current of 20 nA on Ti-rich standards and 200 nA on Ti-poor unknowns; beam spot size 5–10 µm), largely following the procedure of [3]. In-house rutile (for Ti), quartz (for Si), and corundum (for Al) standards were used for calibration, which was then verified with quartz with a known Ti concentration (~215 ppm Ti) [24]. Titanium concentrations were measured on four spectrometers and summed, while Si and Al were monitored on one spectrometer. Counting times were 400 s on peaks and 200 s on adjacent backgrounds. The detection limit for Ti was ~8–10 ppm. We use the TitaniQ calibration of Thomas et al. (2010) [3] (cf. [10]) to derive crystallization (equilibrium) temperatures. While a_{TiO_2} in rutile-crystallizing rocks is 1, felsic rocks without rutile typically have $0.5 < a_{TiO_2} < 1$ [2,3]. All Ti-in-quartz temperature solutions presented here are calculated using a reasonable range of a_{TiO_2} values from 0.5 to 0.8, deemed appropriate for rocks containing quartz that crystallized together with either Ti-magnetite or titanite [25-27].

Results: *Yucatán-6 impact melt rock:* Three (sub-)types of silica were analyzed in the melt rock. The secondary anhydrite- and Ti-magnetite-bearing spherulitic silica vein, in its central part, yielded a mean Ti-in-quartz concentration of 3 ± 8 ppm Ti and 94 ± 35 ppm Al (n=14, with 0 ppm Ti in 12 out of 14 spots, and up to 25 ppm Ti in two additional spots), i.e., Ti was largely below the EMPA detection limit.

The margin of the silica vein also has Ti below detection limit (0 ppm) but 1850 ± 220 ppm Al (*n*=5). Assuming paleopressures of 0.1 kbar ~400 m below the surface of impactite deposits inside the annular moat of the newly formed Chicxulub crater [14,17], calculated Ti-in-quartz crystallization temperatures for the silica vein and its margin range between ~409 and ~270 °C. Recrystallized, locally spherulitic, grains of quartz in the adjacent impact melt groundmass, which were inherited from the target rock and surrounded by pyroxene coronas, have 33 ± 6 ppm Ti and 640 ± 340 ppm Al (*n*=4), indicating an origin different from that of the spherulitic vein.

Expedition 364 suevite: Anhedral quartz in the groundmass of the reworked suevitic breccia, intergrown with calcite and zeolite, yielded Ti below detection limit (1 ± 6 ppm) and 2860 ± 1890 ppm Al (*n*=20/23). Three additional EMPA spots yielded values up to 143 ppm Ti, but we cannot rule out those spot results reflect Ti-rich contamination. Similar to the results for the Y-6 melt rock, and assuming a paleopressure of 0 kbar near the crater surface soon after the time of impact, Ti-in-quartz temperatures derived from the suevite sample range from ~407 to ~268 °C.

Expedition 364 peak-ring granitoid rocks: All target rock samples analyzed yielded similar mean Ti-in-quartz concentrations: granitoid rock from 887 mbsf has 30 ± 11 ppm Ti and 38 ± 17 ppm Al (*n*=10); granitoid rock from 949 mbsf has 30 ± 29 ppm Ti and 56 ± 54 ppm Al (*n*=8/10, with 2 additional spot results ≤150 ppm Ti); granitoid rock from 1133 mbsf yielded 36 ± 17 ppm Ti and 20 ± 12 ppm Al (*n*=11/12, with 115 ppm Ti in one spot); and granitoid rock from 1250 mbsf yielded 37 ± 41 ppm Ti and 118 ± 172 ppm Al (*n*=26/27, with ~450 ppm Ti in one spot). Because the crystalline peak-ring lithologies had been sitting at a depth of ~8–10 km before they were uplifted by the Chicxulub impact [22], paleopressures for crystallization are estimated to have ranged between ~2.2 and ~2.7 kbar. Combined with the range of 30 to 37 ppm Ti, this suggests equilibrium temperatures for quartz in the granitoid rocks were ~561 to ~495 °C [3].

Discussion: Titanium-in-quartz crystallization temperatures in the Chicxulub samples reflect both pre-impact and syn- to post-impact processes. Temperatures obtained from the Y-6 sample suggest the spherulitic silica vein that cross-cuts the impact melt rock formed during relatively high-temperature (≥270 °C) post-impact hydrothermal activity inside the crater moat [18,19]. Anhydrite in that vein (Fig. 1) is also a hydrothermal phase, in agreement with previous reports of vein- and cavity-filling anhydrite in impactites from the Y-6 borehole [15,16]. However, due to the low concentration of Ti below the EMPA detection limit, those temperatures are not very well constrained, and the effects of rapid, non-equilibrium growth of spherulitic silica on either exclusion [4] or entrapment [10] of Ti are currently debated. Quartz in the Expedition 364 suevite sample likely precipitated at temperatures similar to those obtained from the Y-6 sample.

Ti-in-quartz temperature estimates (and Al-in-quartz) are relatively uniform for all target rock samples analyzed. Thus, even over a relatively wide range of depths within core M0077A (887 to 1250 mbsf), equilibrium conditions for the granitoid bodies during the Paleozoic appear to have been similar. It seems reasonable to assume that shock metamorphism (i.e., shock pressures of ~12.5 to 17.5 GPa [28] and post-shock heating adding some 100 to 150 °C to the heat budget [29]) did not notably alter or 'reset' the Ti-in-quartz systematics in these samples. Calculated equilibrium temperatures for the granitoid target rock samples of ~561 to 495 °C may appear low, but are similar to recent Ti-in-quartz temperature estimates for granites [8]. Based on our Ti-(and Al-)in-quartz results, the target rock samples from Chicxulub's peak ring may have been derived from the same pluton or group of plutons that intruded the Maya Block [14] around 340 Ma [30].

References: [1] Wark D. A. and Watson E. B. (2006) *Contrib. Mineral. Petrol., 152,* 743–754. [2] Hayden L. A. and Watson E. B. (2007) *EPSL, 258,* 561–568. [3] Thomas J. B. et al. (2010) *Contrib. Mineral. Petrol., 160,* 743–759. [4] Thomas J. B. and Watson E. B. (2012) *Contrib. Mineral. Petrol., 164,* 369–374. [5] Thomas J. B. et al. (2015) *Contrib. Mineral. Petrol., 169,* 27, 16 pp. [6] Ashley K. T. et al. (2013) *G^3, 14,* 3821–3843. [7] Ashley K. T. et al. (2014) *Am. Mineral., 99,* 2025–2030. [8] Ackerson M. R. et al. (2018) *Nature, 559,* 94–97. [9] Wilson C. J. et al. (2012) *Contrib. Mineral. Petrol., 164,* 359–368. [10] Huang R. and Audétat A. (2012) *GCA, 84,* 75–89. [11] Naumov M. V. (2005) *Geofluids, 5,* 165–184. [12] Watson E. B. et al. (2006) *Contrib. Mineral. Petrol. 151,* 413–433. [13] Kenny G. G. et al. (2016) *Geology, 44,* 435–438. [14] Kring D. A. (2005) *Chem. d. Erde, 65,* 1–46. [15] Kring D. A. and Boynton W. V. (1992) *Nature, 358,* 141–144. [16] Schuraytz B. C. et al. (1994) *Geology, 22,* 868–872. [17] Sharpton V. L. et al. (1996) *GSA Spec. Pap., 307,* 55–74. [18] Abramov O. and Kring D. A. (2007) *MAPS, 42,* 93–112. [19] Zürcher L. and Kring D. A. (2004) *MAPS, 39,* 1199–1221. [20] Ames D. E. et al. (2004) *MAPS, 39,* 1145–1167. [21] Kring D. A. et al. (2017) *LPS XLVIII,* abstr. #1212. [22] Morgan J. V. et al. (2016) *Science, 354,* 878–882. [23] Gulick S. P. S. et al. (2017) Exp. 364 Prelim. Rep., IODP, 38 pp. [24] Robinson K. L. (2015) Ph.D. thesis, Univ. Hawai'i, 112 pp. [25] Pan L.-C. et al. (2018) *Am. Mineral., 103,* 1417–1434. [26] Wang S.-J. et al. (2018) *J. Metam. Geol., 35,* 601–629. [27] Turnbull R. E. et al. (2013) *New Zealand J. Geol. Geophys., 56,* 83–99. [28] Rae A. S. P. et al. (2017) *LPS XLVIII,* abstr. #1934. [29] Stöffler D. (1984) *J. Non-Cryst. Solids, 67,* 465–502. [30] Schmieder M. et al. (2017) 80th MetSoc, abstr. #6134.